Impact on Catalysis of Secondary Structural Manipulation of the αC-Helix of *Escherichia coli* Dihydrofolate Reductase†

Luyuan Li and Stephen J. Benkovic*

Department of Chemistry, 152 Davey Laboratory, The Pennsylvania State University, University Park, Pennsylvania 16802

Received July 31, 1990; Revised Manuscript Received November 7, 1990

ABSTRACT: The αC-helix of *Escherichia coli* dihydrofolate reductase has been converted to its counterpart in *Lactobacillus casei* by a triple mutation in the helix (H45R, W47Y, and I50F). These changes result in a 2-fold increase in the steady-state reaction rate (k_{cat} = 26 s^{-1}) that is limited by an increased off rate for the release of tetrahydrofolate (k_{off} = 40 s^{-1} versus 12 s^{-1}). On the other hand the mutant protein exhibits a 10-fold increase in the K_M value (6.8 μM) for dihydrofolate and a 10-fold decrease in the rate of hydride transfer (85 s^{-1}) from NADPH to dihydrofolate. The elevated rate of tetrahydrofolate release upon the rebinding of NADPH, a characteristic of the wild-type enzyme-catalyzed reaction, is diminished. The intrinsic pK_a (6.4) of the mutant enzyme binary complex with NADPH is similar to that of the wild type, but the pK_a of the ternary complex is increased to 7.3, about one pH unit higher than the wild-type value. Further mutagenesis (G51P and an insertion of K52) was conducted to incorporate a hairpin turn unique to the C-terminus of the αC-helix of the *L. casei* enzyme in order to adjust a possible dislocation of the new helix. The resultant pentamutant enzyme shows restoration of many of the kinetic parameters, such as k_{cat} (12 s^{-1}), K_M (1.1 μM for dihydrofolate), and k_{hyd} (526 s^{-1}), to the wild-type values. The synergism in the product release is also largely restored. A substrate-induced conformational change responsible for the fine tuning of the catalytic process was found to be associated with the newly installed hairpin structure. The Asp27 residue of the mutant enzyme was found to be reprotonated before tetrahydrofolate release.

Dihydrofolate reductase (DHFR)[1] (5,6,7,8-tetrahydrofolate: $NADP^+$ oxidoreductase) catalyzes the reduction of dihydrofolate (H_2F) by NADPH to form 5,6,7,8-tetrahydrofolate (H_4F). DHFR has been the subject of extensive structural and kinetic studies: the structures of the *Escherichia coli* and *Lactobacillus casei* enzymes have been determined to 1.7-Å resolution for some binary and ternary complexes (Bolin et al., 1982; Filman et al., 1982; Bystroff et al., 1990), and their complete kinetic schemes have been derived from pre-steady-state and steady-state kinetics (Fierke et al., 1987; Andrews et al., 1989). Despite a primary amino acid sequence homology of 28%, the tertiary structure of the two enzymes shows a remarkable similarity: the solvent-accessible surface of methotrexate (MTX) in the binary complexes of the *E. coli* and *L. casei* DHFRs is identical (±2%), and the solvent-accessible active-site surface of the *E. coli* enzyme is 93% of that of the *L. casei* enzyme (Benkovic et al., 1988). Consistent with the similarities in protein–substrate interactions, the overall kinetic schemes of the two enzymes are identical in terms of the number, arrangement, and magnitude of the kinetic steps. Site-directed mutagenesis of the *E. coli* DHFR combined with detailed kinetic analysis has been utilized to probe specific structural–functional relationships, in particular, the role of conserved individual amino acid residues involved in enzyme–substrate interactions (Villafranca et al., 1983; Chen et al., 1985, 1987; Howell et al., 1986; Mayer et al., 1986; Taira et al., 1987; Taira & Benkovic, 1988; Appleman et al., 1988, Fierke & Benkovic, 1989; Adams et al., 1989; Murphy & Benkovic, 1989).

In the present work, we sought a fresh approach to the study of structural–functional relationships by focusing upon the implications of manipulation of secondary structure, such as replacing one part of *E. coli* DHFR with its counterpart from *L. casei* DHFR. The αC-helix (Volz et al., 1982) was chosen because it (a) has an important role in the formation of the active-site cavity, (b) shows little structural interaction with other parts of the enzyme, and (c) is significantly different in primary sequence between the *E. coli* and the *L. casei* enzymes. Site-directed mutagenesis was conducted to produce two mutant enzymes. The first mutant enzyme involves the replacement of the αC-helix of the *E. coli* enzyme with that of the *L. casei* enzyme. The second mutant enzyme results from incorporation of a hairpin structure (Bolin et al., 1982) that is present at the end of the αC-helix of the *L. casei* enzyme but is absent from the *E. coli* enzyme at the same position. The two mutant enzymes were then subjected to steady-state and pre-steady-state kinetic studies to examine the impact of these considerably large changes in secondary structure on the catalytic behavior.

Materials and Methods

Materials

Dihydrofolate was prepared by the reduction of folate by using the method of Blakley (1960). (6*S*)-Tetrahydrofolate was prepared by using wild-type dihydrofolate reductase to reduce H_2F (Mathews & Huennekens, 1963) and purified on DE-52 resin by eluting with a trimethylammonium bicarbonate linear gradient (Curthoys et al., 1972). [4′(*R*)-^{2}H]NADPH

† This work was supported by an NIH Grant GM24129.

* To whom all correspondence should be addressed.

[1] Abbreviations: DHFR, dihydrofolate reductase; H_2F, 7,8-dihydrofolate; H_4F, 5,6,7,8-tetrahydrofolate; NADPH or NH, nicotinamide adenine dinucleotide phosphate, reduced; $NADP^+$ or N, nicotinamide adenine dinucleotide phosphate; MTX, methotrexate; DAM, 2,4-diamino-6,7-dimethylpteridine; RYF, a mutant *E. coli* DHFR that bears three mutations His45 → Arg (H45R), Trp47 → Tyr (W47Y), and Ile50 → Phe (I50F); PKRP, a mutant *E. coli* DHFR that bears five mutations, H45R, W47Y, I50F, Gly51 → Pro (G51P) and an insertion of Lys52 (K52).

0006-2960/91/0430-1470$02.50/0 © 1991 American Chemical Society

was prepared by using *Leuconostoc mesenteroides* alcohol dehydrogenase (Stone & Morrison, 1982) obtained from Research Plus Inc. and then purified by the method of Viola et al. (1979). The concentrations of the substrates were determined as described (Fierke et al., 1987). Methotrexate was purchased from Sigma and its concentration was determined in 0.1 M NaOH spectrophotometrically by using a molar extinction coefficient of 22 100 M^{-1} cm^{-1} at 302 nm (Seeger et al., 1949). 2,4-Diamino-6,7-dimethylpteridine (DAM) was purchased from ICN Pharmaceuticals and its concentration was determined spectrophotometrically at pH 6.0 at 346 nm by using a molar extinction coefficient of 6900 M^{-1} cm^{-1} (Brown & Jacobson, 1961).

Plasmids pRWa1 and pRWc1, both of which carry the DHFR gene (*fol*) and an overexpression promoter, and are ampicillin or chloramphenicol resistant, respectively (C. R. Wagner and S. J. Benkovic, personal communication), were gifts from Dr. C. R. Wagner of this laboratory. Oligonucleotides were prepared at the Biotechnology Institute at The Pennsylvania State University.

Endonucleases and mung bean nuclease were purchased from New England Biolabs. T4 DNA ligase was purchased from IBI. *E. coli* DNA polymerase I (Klenow fragment) was prepared in this laboratory.

Methods

Incorporation of Unique Restriction Sites. Two unique restriction endonuclease sites, Nar I and Eag I, were introduced into the *fol* gene at positions that flank the codons encoding the αC-helix of the *E. coli* DHFR by oligonucleotide-directed mutagenesis, using the gapped-duplex DNA method, basically as described (Kramer & Fritz, 1987). About 0.2 μg of single-stranded, cyclic DNA prepared from pRWa1 was annealed in 12.5 mM Tris/0.2 mM KCl (pH 7.5) to about 2 μg of linearized, denatured DNA prepared from pRWc1 by *Cla*I and *Sma*I restriction endonuclease digestion. The resultant gapped-duplex DNA was then hybridized with a 49-base oligonucleotide, 5′-CCGTGATTAT GGGGCGCCAT ACCTGGGAAT CAATCGGCCG TCCGTTGCC-3′, which contains the sequences for *Nar*I and *Eag*I restriction sites (underlined), and the gaps were filled and ligated in a solution that contained 27.5 mM Tris-HCl (pH 7.5), 62.5 mM KCl, 15 mM $MgCl_2$, 2.0 mM dithiothreitol, 0.05 mM ATP, 0.025 mM each of dATP, dTTP, dGTP, and dCTP, T4 DNA ligase (4 units), and DNA polymerase I (Klenow fragment; 1 unit) at 25 °C for 45 min. The gap-filled DNA was used to transform *E. coli* (strain BMH71-18, mut S) cells by the method of Hanahan (1983). Segregation of the transformed cells was performed on plates of Luria-Bertani medium that contained chloramphenicol (25 μg/mL) and trimethoprim (10 μg/mL). Plasmid DNA containing the desired mutation was selected by *Nar*I and *Eag*I digestions and confirmed by full sequencing of the gene by the general method of Sanger (1981). The selected plasmid was labeled as pLLc1-1.

Cassette-Directed Mutagenesis. In order to insert between *Nar*I and *Eag*I sites an oligonucleotide cassette that carries three mutations to the *E. coli* DHFR, H45R, W47Y, and I50F, pLLc1-1 DNA was subjected to *Nar*I and *Eag*I digestion. The larger DNA fragment was isolated by an agarose gel/DEAE membrane procedure as described (Winberg & Hammarskjold, 1980). The fragment DNA was ligated, as described (Legerski & Robbertson, 1985), to a double-stranded DNA obtained by annealing two synthetic oligonucleotides, 5′-CGGCGCACCT ATGAAAGTT C-3′ and 5′-GGCCGAAACT TTCATAGGTG CGC-3′, which gives sticky ends (underlined) compatible to those generated by *Nar*I and *Eag*I digestion. The ligation product was then used to transform *E. coli* (strain w71-18) cells. The desired mutant was selected by the presence of an *Eag*I site but the absence of an *Nar*I site and confirmed by full DNA-sequencing. The selected plasmid was labeled as pLLc2-2.

In order to insert a cassette that carries five mutations in *E. coli* DHFR, H45R, W47Y, I50F, G51P, and an insertion of K52, plasmid pLLc1-1 was digested with *Eag*I endonuclease. After purification, the linearized DNA was digested with mung bean nuclease (Kroeker et al., 1976) in a solution that contained 50 mM sodium acetate (pH 5.3), 30 mM NaCl, 1 mM $ZnCl_2$, and the enzyme (20 units) at 30 °C for 30 min. The resultant blunt-ended DNA was then digested with *Nar*I endonuclease. The larger fragment of the resultant DNA was purified and ligated to a double-stranded DNA obtained from annealing two synthetic oligonucleotides, 5′-CGCCGCACAT ATGAAAGTTT TCCTAAAC-3′ and 5′-GTTTAGGAAA ACTTTCATAT GTGCGG-3′, which contains a blunt end and a sticky end (underlined) compatible to that generated by *Nar*I digestion. The ligation product was used to transform *E. coli* (strain MK30-3) cells. The desired mutant was selected by the presence of an *Nde*I site (5′-CATATG-3′) carried by the newly incorporated oligonucleotides and confirmed by full sequencing of the gene. The selected plasmid was labeled pLLc3-4.

Enzyme Purification. The mutant dihydrofolate reductases were purified, basically as described (Chen et al., 1987), from the corresponding *E. coli* strains by using a MTX affinity resin. Both mutant enzymes were eluted from the MTX resin with borate buffer (pH 9.0) containing 0.5 mM folate. Each enzyme solution was then dialyzed and further purified through a DEAE-Sephacel column. The enzyme concentrations were determined by MTX titration (Williams et al., 1979).

Stopped-Flow and Kinetic Measurements. Unless otherwise indicated, all kinetic and equilibrium measurements were conducted at 25 °C in a buffer that contained 50 mM 2-(*N*-morpholino)ethanesulfonic acid, 25 mM Tris, 25 mM ethanolamine, and 100 mM NaCl (MTEN buffer, pH 5–10). Some experiments were conducted, as indicated, in a buffer in which the 2-(*N*-morpholino)ethanesulfonic acid of MTEN buffer is replaced with 50 mM sodium acetate (STEN buffer, pH 5–8). Over the pH range used, the ionic strength of this buffer remains constant (Ellis & Morrison, 1982). Pre-steady-state data were obtained as described (Fierke et al., 1987) by using a stopped-flow apparatus built in the laboratory of Johnson (1986). Initial velocities were determined by monitoring the rate of enzyme-dependent absorbance decrease at 340 nm with a molar extinction coefficient of 11 800 M^{-1} cm^{-1} on a Cary 219 spectrophotometer. The enzyme was preincubated with either NADPH or H_2F for 2–3 min to remove hysteretic behavior (Penner & Frieden, 1985). The association and dissociation rate constants were determined by stopped-flow fluorescence quenching as described (Dunn & King, 1980; Cayley et al., 1981). Equilibrium dissociation constants were measured as described (Birdsall et al., 1980; Stone & Morrison, 1982).

Data Analysis. Data obtained at each pH value by varying the substrate concentration (S) were fitted to eq 1 by a non-

$$v = VS/(K_M + S) \quad (1)$$

linear regression program to yield maximum velocity (V) and the Michaelis constant (K_M). Unless otherwise indicated, the pH profiles were fitted to eq 2 where C is the pH-independent

$$y = C/(1 + K_a/H) \quad (2)$$

kinetic parameter, K_a is an acid dissociation constant, and H

Table I: Amino Acid Sequences of the Mutant DHFRs with Respect to αC-Helices

enzyme	αC[a]	enzyme	αC[a]
E. coli	[43]GRHTWESIG-RPL	PKRP	GRRTYESFPKRPL
RYF[b]	GRRTYESFG-RPL	*L. casei*	GRRTYESFPKRPL

[a] *E. coli* numbering system is used. [b] Underlined characters indicate mutation sites.

Table II: Steady-State Parameters[a]

	k_{cat} (s^{-1})	$K_M(H_2F)$ (μM)	pK_a[b]	^DV (pH 6.0)	^DV (pH 9.0)
RYF	26.3 ± 1.1	6.8 ± 0.1	6.4 ± 0.1	2.1 ± 0.3	3.1 ± 0.4
PKRP	12.2 ± 1.5[c]	1.1 ± 0.1	6.6 ± 0.1	1.0 ± 0.1	1.7 ± 0.1
E. coli	12[d]	<1[d]	6.5[d]	1.0[e]	2.9[e]
L. casei[f]	31	1	6.0	1.1	2.7

[a] Experimental conditions are identical with those described in the legend to Figures 1 and 2: k_{cat} and $K_M(H_2F)$ values are determined at pH ≤ 6.0 unless otherwise indicated. [b] Determined by the pH dependence of inhibition of DHFR activity by 2,3-diamino-6,7-dimethylpteridine. [c] Observed at pH 7.5. [d] Fierke et al. (1987). [e] Chen et al. (1987). [f] Andrews et al. (1989).

is $[H^+]$. Simulation of the reaction schemes was conducted by using the kinetic simulation program KINSIM (Barshop et al., 1983).

Results

αC-Helices of the Mutant DHFRs. The techniques of site-specific mutagenesis have been employed to produce two mutant *E. coli* DHFRs for the present studies. The amino acid sequences of the mutant enzymes, with regard to the αC-helices (His45 to Ile50, *E. coli*), are given in Table I, in comparison with the αC-helices of the wild-type *E. coli* and *L. casei* DHFRs. In the first mutant enzyme (RYF), a triple mutation (His45 → Arg, Trp47 → Tyr, Ile50 → Phe) was constructed so that the αC-helix of the *E. coli* DHFR was in effect replaced with its counterpart in the *L. casei* DHFR. In the second mutant enzyme (PKRP), two additional site-specific mutations were introduced into the RYF enzyme. Glycine 51 was substituted by a proline residue, which was followed by the insertion of a lysine residue, in order to incorporate a hairpin turn (Bolin et al., 1982) that is found in the *L. casei* DHFR but absent from the *E. coli* enzyme. This extra turn in the *L. casei* DHFR occurs at a point corresponding to a single insertion (Lys51) in the *L. casei* sequence relative to the *E. coli* sequence. There is also a cis peptide bond, found only in the *L. casei* DHFR structure, between Arg52 and Pro53 (Bolin et al., 1982). It is possible that substitution for residues in the αC-helix and the loop structure up to Leu54 of the *E. coli* DHFR with those of the *L. casei* DHFR would lead to the formation of a cis peptide bond at the corresponding position in the PKRP enzyme, although this cannot be confirmed without a structural study.

Steady-State Kinetics. As presented in Table II, the most apparent impact on the steady-state kinetic parameters observed for the RYF enzyme is the Michaelis constant (K_M) for H_2F, which is 6.8 μM in the acidic region (pH ≤ 6) and about 100 μM in the basic region (pH > 8), reflecting a 10- to 100-fold increase when compared with the wild-type values (Stone & Morrison, 1984). The pH-independent k_{cat} is more than twice that for the wild-type *E. coli* DHFR reaction and is similar to that of the *L. casei* DHFR-catalyzed reaction. Analysis of the pH profiles for k_{cat} and k_{cat}/K_M for the RYF enzyme (Figure 1) yields apparent pK_a values of 8.41 ± 0.12 and 7.09 ± 0.12, the latter is about one pH unit less than that for the wild-type *E. coli* DHFR (Stone & Morrison, 1984).

The K_M (H_2F) value for the PKRP enzyme, on the other hand, is about 1 μM in the acidic region (pH ≤ 6) and about

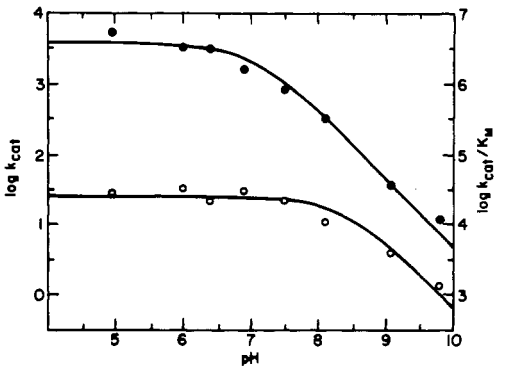

FIGURE 1: pH dependence of k_{cat} (open circles) and $k_{cat}/K_M(H_2F)$ (closed circles) for the RYF enzyme. The data were fitted to eq 2. Experimental conditions were 0.9–47 nM enzyme, 1.2–120 μM H_2F, and 60 μM NADPH, 25 °C. The enzyme was preincubated with NADPH.

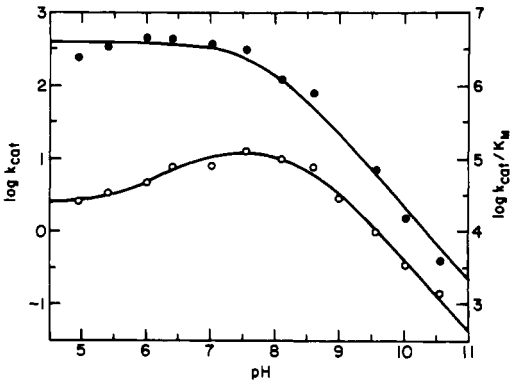

FIGURE 2: pH dependence of k_{cat} and $k_{cat}/K_M(H_2F)$ for the PKRP enzyme. The enzyme (3.6–178 nM) was preincubated with H_2F (0.6–116 μM) at 25 °C for 2–3 min, and then the reaction was initiated by the addition of NADPH (108 μM). The $k_{cat}/K_M(H_2F)$ (closed circles) and k_{cat} (open circles) data were fitted to eqs 2 and 3, respectively.

13 μM in the basic region (pH > 8), reflecting a marked improvement in apparent H_2F binding as a result of the presence of the hairpin turn. The pH profiles for k_{cat} and k_{cat}/K_M for the PKRP enzyme are shown in Figure 2.

The k_{cat} data were best described by eq 3, where K_a and K_b

$$k_{cat} = \frac{(k_{off} + k_{off}'H/K_b)}{(1 + H/K_b)(1 + K_a/H)} \quad (3)$$

are apparent acid dissociation constants and k_{off} and k'_{off} are rate constants for the dissociation of H_4F from the ternary complexes, E·NADPH·H_4F and EH·NADPH·H_4F (see below). Fitting the k_{cat}–pH profile to eq 3 yields k_{off} = 14.1 ± 0.9 s^{-1}, k'_{off} = 2.5 ± 0.2 s^{-1}, pK_b = 6.61 ± 0.24, and pK_a = 8.48 ± 0.10. The optimum reaction rate is at pH 7.5. The k_{cat}/K_M–pH profile (Figure 2) is described by eq 2, where the pK_a = 7.75 ± 0.10.

As noted previously (Penner & Frieden, 1985), DHFR is usually preincubated with either NADPH or H_2F in order to avoid hysteresis. Whereas the RYF enzyme may be preincubated with either H_2F or NADPH, the order of substrate addition has a profound impact on the kinetic behavior of the PKRP enzyme. Thus, when the PKRP enzyme was preincubated with saturating amounts of NADPH for 2–3 min, followed by H_2F addition to start the reaction, a hysteresis in the steady-state reaction rate was observed in the neutral or basic pH region. Upon the addition of H_2F at pH 7.0, the initial reaction rate (1.2 μM/min) increased for about 2 min, until a new equilibrium was reached at which time the reaction

Table III: Thermodynamic Dissociation Constants[a] (pH 6.0)

	K_D (μM)	
	H_2F	NADPH
RYF		1.31 ± 0.12 (1.5 ± 1.1)
PKRP	1.65 ± 0.02 (1.8 ● 0.8)[b]	1.83 ± 0.36 (1.2 ± 0.9)
E. coli	0.22[c]	0.33[c]
L. casei	0.44[d]	0.01[e]

[a] Measured in MTEN buffer at 25 °C. [b] Values in parentheses were estimated from kinetic binding rate constants (see Table IV). [c] Fierke et al. (1987). [d] Birdsall et al. (1980). [e] Andrews et al. (1989).

rate (1.5 μM/min) again became linear. This final rate, measured at 2 min after the addition of H_2F, was slightly less than the initial rate (1.7 μM/min) observed when the enzyme was preincubated with H_2F. There was no difference in the reaction rate in the acidic pH region whether the enzyme was preincubated with NADPH or H_2F. These results suggest that (a) there are two conformers for the PKRP enzyme, one favoring NADPH binding and the other H_2F and (b) the NADPH-stabilized conformer is gradually converted to the H_2F-stabilized conformer after multiple turnovers.

In order to determine the intrinsic pK_a values for the mutant enzyme·NADPH binary complexes, the pH-dependence for binding the competitive inhibitor, 2,4-diamino-6,7-dimethylpteridine (DAM), was measured (Stone & Morrison, 1983; Cleland, 1977). The results are given in Table II. These pK_a values are similar to that for the wild-type *E. coli* DHFR.

Deuterium Isotope Effects on the Reaction Rate. The pH dependence of the deuterium isotope effect on V for the mutant enzyme catalyzed reactions was analyzed by using [4′(*R*)-^{2}H]NADPH (Table II). The ^DV value at pH 6.0 is 2.1 for the RYF enzyme catalyzed reaction, instead of about 1 as it is for the PKRP enzyme as well as wild-type DHFR. This suggests that the hydride-transfer rate in the reaction catalyzed by the RYF enzyme is significantly reduced such that it becomes partially rate-limiting. In the basic region (pH 9.0), the smaller ^DV value for the PKRP enzyme catalyzed reactions relative to the other DHFRs indicates that for the PKRP enzyme the hydride-transfer rate at pH 9.0 is still only partially rate-limiting.

Thermodynamic Dissociation Constants (K_D). The binding of H_2F and NADPH to free DHFR was examined by following the decrease in enzyme fluorescence that occurs upon formation of DHFR–ligand complexes. The K_D values for H_2F and NADPH are given in Table III for the mutant enzymes. Only modest increases in K_D relative to that for the *E. coli* enzyme were observed except for the binding of H_2F to the RYF enzyme, which could not be measured because of very poor fluorescence quenching signals, a result of a much lowered affinity for H_2F.

Substrate Binding. The rates of substrate binding to the mutant DHFR in either the NADPH site or the folate site were determined by monitoring the quenching of intrinsic enzyme fluorescence, using relaxation stopped-flow techniques (Dunn & King, 1980; Cayley et al., 1981). As described by Adams et al. (1989), the ligand-dependent fluorescence

Scheme I

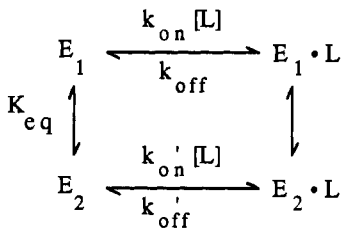

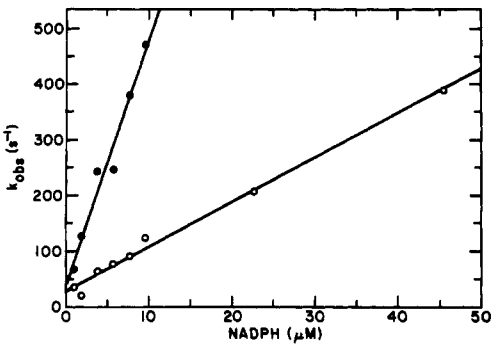

FIGURE 3: Concentration dependence of the observed rate constants (k_{obs}) for the two fast phases of NADPH binding to the PKRP enzyme as measured by relaxation stopped flow. Lines 1 (close circles) and 2 (open circles) correspond to E_1 and E_2 binding, respectively.

quenching observed in the binding of NADPH to the wild-type *E. coli* DHFR is biphasic and each of the two phases corresponds to the binding of the cofactor to one of the two conformers of the enzyme, as illustrated in Scheme I. These phases are followed by a much slower phase that reflects the conversion of E_2 to E_1 (or E_2·NH to E_1·NH).

It was found that ligand binding to the RYF and PKRP enzymes, as revealed by the fast quenching of enzyme fluorescence, is also biphasic. A plot of the k_{obs} values as a function of NADPH concentration is depicted in Figure 3. The association and dissociation rate constants obtained by this method are given in Table IV. The binding of NADPH to the RYF enzyme shows that one of the two enzyme conformers exhibits a higher affinity over the other conformer toward the ligand. The rate of the interconversion of the two conformers for the RYF enzyme is estimated to be 0.03 s^{-1} from the slow phase of the fluorescence quenching (data not shown).

The binding of both H_2F and NADPH to PKRP enzyme exhibits two fast ligand-dependent phases, and the corresponding kinetic binding rate constants indicate that one conformer is preferred over the other in the binding of these ligands (Table IV). It is unknown presently whether NADPH and H_2F exhibit higher affinity toward the same conformer; however, the steady-state data described earlier and pre-steady-state data (see below) indicate that, for the PKRP enzyme, the conformer stabilized by H_2F differs catalytically from the one stabilized by NADPH. The rate of conversion of the conformers is 0.03 s^{-1} as measured from NADPH binding.

Table IV: Binding Constants by the Relaxation Method (pH 6.0)

	H_2F				NADPH			
	k_{on} (μM^{-1} s^{-1})	k_{off} (s^{-1})	k_{on}' (μM^{-1} s^{-1})	k_{off}' (s^{-1})	k_{on} (μM^{-1} s^{-1})	k_{off} (s^{-1})	k_{on}' (μM^{-1} s^{-1})	k_{off}' (s^{-1})
RYF					22.0 ± 2.0	23.9 ± 14.6	9.1 ± 1.1	19.8 ± 8.0
PKRP	53.3 ± 5.2	68.8 ± 23.7	15.8 ± 1.1	45.4 ± 13.4	44.5 ± 4.0	34.0 ± 23.4	8.0 ± 0.3	27.4 ± 5.7
E. coli	42[a]	47[a]			20[b]	3[b]	5[b]	70[b]
L. casei	14	5			14	0.1		

[a] Fierke et al. (1987). [b] Adams et al. (1989). [c] Andrews et al. (1989).

Table V: Dissociation Constants by the Competition Method (pH 6.0)

ligand	enzyme species	trapping ligand	k_{off} (s^{-1}) RYF	PKRP	*E. coli*[a]	*L. casei*[b]
NH	E·NH	N	32.0 ± 1.1	45.4 ± 2.0	3.6	0.1
H_2F	E·H_2F	MTX	201 ± 15	106 ± 14	22	3.7
N	E·N·H_4F	NH	296 ± 33	199 ± 9	200	290
H_4F	E·H_4F	MTX	27.8 ± 2.3	3.8 ± 0.1	1.4	0.5
	E·NH·H_4F	MTX	39.6 ± 3.4	11.0 ± 0.3	12	40
	E·N·H_4F	MTX	28.0 ± 1.3	5.1 ± 0.3	1.7	2.4

[a] Fierke et al. (1987). [b] Andrews et al. (1989).

Scheme II

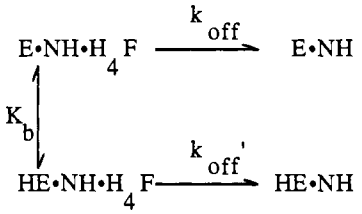

The relationship between the kinetic binding data and the thermodynamic binding data, according to Scheme I, is given by eq 4, where K_i and K_i' represent the ratios of k_{off}/k_{on} and

$$K_D = K_i(1 + 1/K_{eq})/(1 + K_i/K_i'K_{eq}) \quad (4)$$

k_{off}'/k_{on}' for E_1 and E_2, respectively, and K_{eq} is the equilibrium constant ($K_{eq} = E_1/E_2$) determined from the amplitudes of the two fast phases observed in relaxation experiments. The value of K_{eq} for both mutant DHFRs, as inferred from the ratio of the amplitudes of the two fast phases in the fluorescence quenching, is about 1. Estimations of K_D values from the kinetic binding data, using eq 4, are in good agreement with those determined by fluorescence quenching (Table III), with the major source of errors being the measurement of k_{off} values by the relaxation method.

Ligand Dissociation Rates by a Competition Method. An independent measure of the dissociation rate constants (k_{off}) may be obtained by a competition method (Birdsall, 1980). The dissociation rate constants for the substrates and products of the reactions catalyzed by the mutant enzymes are presented in Table V. For the RYF enzyme, the off rates for both NADPH and H_2F are about 10-fold larger than those for the wild-type *E. coli* DHFR. The large k_{off} value for H_2F is consistent with the low signals for fluorescence quenching as mentioned above. For the PKRP enzyme, there is also a 10-fold increase in k_{off} for NADPH, but k_{off} for H_2F is one-half of that with the RYF enzyme. The k_{off} values obtained by the competition method are similar to those measured by the relaxation method for the conformer that shows higher affinity toward NADPH or H_2F.

The off rate of H_4F in the E·NH·H_4F ternary complex for the PKRP enzyme is pH-dependent, varying from 3.6 s^{-1} at pH 5.0 to 19.4 s^{-1} at pH 8.0 (curve 2, Figure 4). The pH dependence of the off rate of H_4F can be described by Scheme II, where K_b is the acid dissociation constant of the E·NH·H_4F ternary complex. The observed off-rate constant, k_{obs}, is therefore given in eq 5, where k_{off} and k_{off}' are the off-rate

$$k_{obs} = (k_{off} + k_{off}'H/K_b)/(1 + H/K_b) \quad (5)$$

constants for H_4F in the unprotonated and protonated ternary complexes, respectively. The dissociation rate data gave k_{off} = 20 ± 0.8 s^{-1}, k_{off}' = 3.5 ± 0.3 s^{-1}, and pK_b = 6.60 ± 0.16 (curve 2, Figure 4). The pK_b and k_{off} values are similar to those obtained from the steady-state k_{cat}–pH profile (Figure 2), thus confirming that the pH dependence of H_4F dissociation is apparently responsible for the decline of the reaction rate in the acidic pH region.

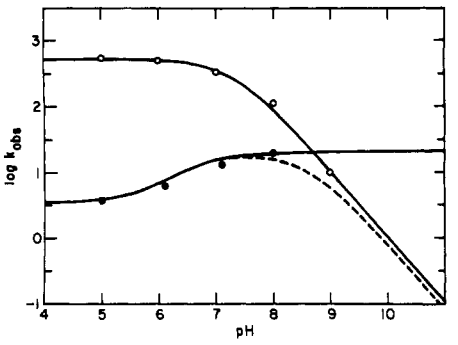

FIGURE 4: Curve 1 (open circles): Observed hydride transfer rate as a function of pH for the PKRP enzyme. The PKRP enzyme was preincubated with H_2F for 2 min, and the reaction was initiated by mixing E·H_2F with NADPH. Final concentrations were 1.33 μM enzyme, 95 μM H_2F, and 102 μM NADPH, pH 6.0, 25 °C. The data were fitted to the equation $k_{obs} = k_{hyd}/(1 + K_a/[H^+])$, where k_{hyd} = 526 ± 22 s^{-1} and pK_a = 7.3 ± 0.1. Curve 2 (closed circles): Observed off rate of H_4F from E·NH·H_4F complex, measured by the competition method using MTX as the chasing ligand. Final concentrations were 5.44 μM enzyme, 75 μM H_4F, 88 μM NADPH, and 350 μM MTX, 25 °C in STEN buffer. The data were fitted to eq 5. Curve 3 (dashed lines): A theoretical line using eq 3 and the results of computer simulation of Scheme IV; the constants used for the simulation are $k_1 = 1 \times 10^7$ M^{-1} s^{-1}, k_2 = 10 s^{-1}, k_3 = 500 s^{-1}, $k_4 = 5 \times 10^{-3}$ s^{-1}, $k_7 = 1 \times 10^7$ M^{-1} s^{-1}, k_8 = 50 s^{-1}, K_9 = 100, k_{11} = 20 s^{-1}, k'_{11} = 3.5 s^{-1}, pK_1 = 6.6, pK_2 = 7.3, and pK_3 = 6.6.

Table VI: Rate Constants for Hydride Transfer (k_{hyd})

RYF	PKRP
84.1 ± 8.5[a]	485 ± 29[c]
29.8 ± 1.4[b]	189 ● 11[d]
	165 ± 13[a]
	55 ± 5[b]

[a] NADPH, pH 6.0 (preincubation with NADPH). [b] NADPD, pH 6.0 (preincubation with NADPD). [c] NADPH, pH 6.0 (preincubation with H_2F). [d] NADPD, pH 6.0 (preincubation with H_2F).

An interesting characteristic of the mechanism of the DHFR-catalyzed reactions is synergism in product release (Fierke et al., 1987; Andrews et al., 1989), namely, the off rate of H_4F is accelerated by replacement of $NADP^+$ by NADPH to form E·NH·H_4F. Such synergism is diminished in the RYF enzyme but largely restored in the PKRP enzyme to an extent comparable to the wild-type DHFR's (Table V).

Hydride Transfer. The rate constants for hydride transfer from NADPH to H_2F can be determined from the burst of product formation measured in pre-steady-state experiments (Fierke et al., 1987). In studies with the RYF mutant DHFR, the enzyme was preincubated with NADPH or NADPD and diluted 2-fold into a solution of H_2F to initiate the reaction, which was monitored by stopped-flow fluorescence energy transfer or absorbance changes. The experiments were conducted at acidic or neutral pH, not at basic pH because of the increased K_M value, to ensure that the enzyme would be saturated by substrate. The rate constants for the burst at

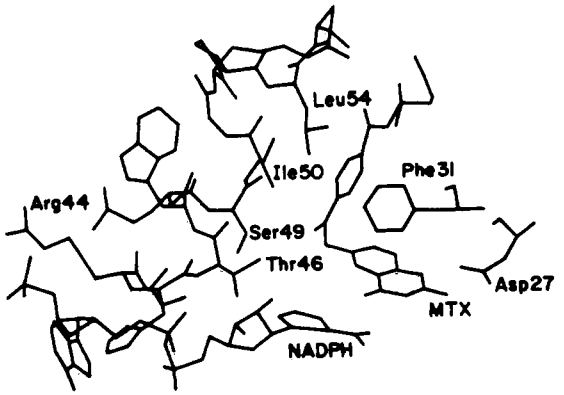

FIGURE 5: Active site of *E. coli* DHFR. The αC-helix and part of a loop structure that follows are shown with respect to bound NADPH and MTX.

pH 6.0 for NADPH and for NADPD are given in Table VI, providing a deuterium isotope effect of 2.8 ± 0.3 (pH 6.0). Similar results were obtained when the enzyme was preincubated with H_2F instead of NADPH. A pK_a of 7.3 and a pH-independent rate constant of 86.4 ± 15.3 for k_{hyd} can be estimated from the dependency of the hydride-transfer rate on pH (data not shown).

Since the steady-state and kinetic binding data on the PKRP enzyme indicate the presence of two active conformers, the pre-steady-state study on this mutant DHFR was also conducted in two different ways. In one set of experiments, the PKRP enzyme was preincubated with H_2F and diluted into NADPH or NADPD solution to initiate the reaction, which was monitored by absorbance decrease (by using a 340-nm filter) due to the disappearance of NADPH or NADPD and H_2F. These data were fitted with an equation that describes a single-exponential decay that represents rapid product formation, followed by a linear decrease of the absorbance that corresponds to the steady-state turnover. The observed rate constants for initial product formation at pH 6.0 for NADPH and for NADPD are listed in Table VI and gave rise to a deuterium isotope effect on hydride transfer of 2.6 ± 0.2. The relative amplitude of this pre-steady-state phase was 0.81 measured in the acidic pH region. The pH dependence of k_{hyd} (Figure 4) gives a pH-independent rate constant of 526 ± 22 s^{-1} and a pK_a for the E·NH·H_2F ternary complex of 7.3 ± 0.1.

In another set of experiments, the PKRP enzyme was preincubated with NADPH or NADPD, instead of H_2F. The rate constants for the burst at pH 6.0 for NADPH and for NADPD were significantly lower than those obtained from experiments in which the enzyme was preincubated with H_2F and gave rise to a deuterium isotope effect for hydride transfer of 3.0 ± 0.4. The relative amplitude of the burst was about 0.74 at pH 5.0. The pH profile for k_{hyd} gives a pH-independent rate constant of 165 ± 16 s^{-1} and pK_a = 7.3 ± 0.2 (data not shown).

Discussion

Both of the αC-helices of *E. coli* and *L. casei* DHFRs are composed of six amino acid residues (Figure 5). According to X-ray crystallographic studies (Bolin et al., 1982; Filman et al., 1982), the active site of both proteins is a cavity about 15 Å deep that is lined by hydrophobic side chains. NADPH binds in an extended conformation with the nicotinamide moiety inserted through the entrance of the cavity. Methotrexate binds in an open conformation with the pteridine ring nearly perpendicular to the benzoyl ring. The pyrimidine edge of the pteridine ring penetrates into the center of the active site where it interacts with Asp27 (*E. coli*) or Asp26 (*L. casei*) through hydrogen bonding. Threonine 46 (*E. coli*) or Thr45 (*L. casei*), which is conserved in all known DHFR sequences, maintains a hydrophobic interaction with the nicotinamide moiety of NADPH. Another highly conserved residue is Ser49 (*E. coli*) or Ser48 (*L. casei*), found in all known DHFR sequences except for *Streptococcus faecium* DHFR, which interacts with the N10-methyl of MTX and with the nicotinamide mononucleotide-ribose through hydrogen bonding mediated by a H_2O molecule. The side chain of Ile50 (*E. coli*) or Phe49 (*L. casei*) is in van der Waals contact with the *p*-aminobenzamide moiety of MTX. Near the N-terminus of the αC-helix, Arg44 (*E. coli*) or Arg43 (*L. casei*) forms an ion pair with the 5′-phosphate of the adenosine mononucleotide as well as a hydrogen bond to the ribose of the adenosine mononucleotide via water. Leucine 54, which is located in the loop structure that follows the αC-helix and is conserved in all known DFHR sequences, interacts hydrophobically with the *p*-aminobenzamide moiety of MTX and is critical in optimizing the rate of hydride transfer (Murphy & Benkovic, 1989). Thus, the αC-helix plays an important role in the formation of the DHFR active-site cavity.

Scheme III

$$E{\cdot}NH{\cdot}H_2F \xrightarrow{k_{HYD}} E{\cdot}N{\cdot}H_4F \xrightarrow{k_9} E{\cdot}NH{\cdot}H_4F \xrightarrow{k_{11}} E{\cdot}NH$$

As a result of the replacement of the αC-helix of *E. coli* DHFR with that of *L. casei* DHFR, the pH-independent k_{cat} (26 s^{-1}) for the RYF enzyme catalyzed reaction is more than twice that of the wild-type *E. coli* DHFR-catalyzed reaction (12 s^{-1}) and approaches that of *L. casei* DHFR (31 s^{-1}). The k_{cat}/K_M (H_4F) value, however, has decreased markedly because of an approximately 10-fold increase in the K_M (H_2F) value. In accord with the much poorer binding of H_2F to the RYF enzyme, the rate of the hydride-transfer step in the E·NH·H_2F ternary complex is reduced to about one-tenth of that observed in the wild-type *E. coli* DHFR reaction (84 s^{-1} versus 950 s^{-1}). The lowered hydride-transfer rate also accounts for the greater deuterium isotope effect on k_{cat} at pH 6.0 (^DV = 2.1).

The increase in k_{cat} directly reflects an increased rate of the release of H_4F (Table V) from E·NH·H_4F that is approximately 3-fold greater than that observed for *E. coli* DHFR and comparable to that for *L. casei* DHFR. Using the abbreviated kinetic process described in Scheme III and substituting k_9 and k_{11} with the k_{off} values for $NADP^+$ and H_4F from the product ternary complexes (Table V), the value of the pH-independent k_{cat} is calculated to be 24.6 ± 5.7 s^{-1}, in close agreement with the observed steady-state value of 26.3 ± 1.1 s^{-1}.

The pK_a value of the E·NH binary complex, pK_1 = 6.4, assigned to Asp27 is unchanged when compared with that of the wild-type *E. coli* enzyme (pK_1 = 6.5; Fierke et al., 1987). The intrinsic pK_a value of the E·NH·H_2F ternary complex, however, increases from pK_2 = 6.5 (wild type; Fierke et al., 1987) to pK_2 = 7.3, in accordance with the differential binding of H_2F to the protonated and unprotonated species of the E·NH binary complex. The relationships between the intrinsic pK_a and those observed in the pH profiles follows from expanding the above kinetic sequence to allow for the influence of pH (Scheme IV). The apparent pK_a values obtained from the k_{cat}/K_M and k_{cat} data are related to the corresponding intrinsic pK_a by pK_a(obs) = pK_1 + log(1 + k_3/k_2) and pK_a(obs) = pK_2 + log(1 + k_3/k_{11}), where k_3 is the hydride-transfer rate constant. When the value of k_2, which was not measured directly, is replaced with the k_{off} value for H_2F in the E·H_2F binary complex, the apparent pK_a values predicted from these

Scheme IV

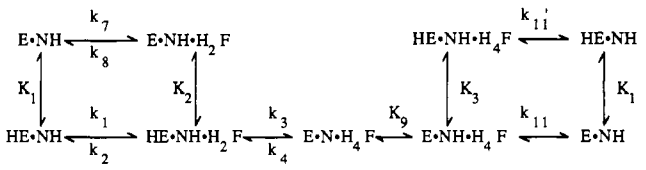

relationships are 6.6 for the k_{cat}/K_M–pH profile and 7.8 for the k_{cat}–pH profile, in fair agreement with the experimentally obtained values, $pK_a(k_{cat}/K_M)$ = 7.1 and $pK_a(k_{cat})$ = 8.4.

One unusual characteristic of the DHFR-catalyzed reaction is the synergism with regard to the release of H_4F, that is, the rate constant for the release of H_4F from the E·NH·H_4F ternary complex is greater than that from E·H_4F or E·N·H_4F. The reaction thus proceeds by an "interlocked" mechanism in which E·NH is the predominant species during steady-state turnover (Fierke et al., 1987; Andrews et al., 1989). Such synergism is not as significant in the RYF enzyme-catalyzed reaction since the dissociation rate constant for H_4F from E·NH·H_4F is only slightly higher than those from E·H_4F and E·N·H_4F complexes (Table V).

All these changes indicate a suboptimal active-site ensemble of the RYF enzyme, resulting probably from a subtle dislocation of the newly incorporated αC-helix. Such dislocation most likely arises from a structural inadequacy at the termini of the α-helix. Since an apparent difference between *E. coli* and *L. casei* DHFRs, with regard to the topology of the αC-helix, is the hairpin turn present only at the C-terminus of the *L. casei* αC-helix, we incorporated elements for the hairpin turn into the RYF enzyme.

This structural change has brought remarkable improvements in activity to the resultant PKRP enzyme. The K_M (H_2F) value in the acidic pH region is about 1 μM, much closer to the wild-type value. The restoration of H_2F binding is also reflected in the k_{on} and k_{off} values for H_2F. In the alkaline pH region, K_M (H_2F) for the PKRP enzyme is about 13 μM, which is about one-eighth of that for the RYF enzyme in the same pH region. The pH dependence of K_M (H_2F) is again directly related to the differential binding of H_2F to the protonated and unprotonated binary complex (pK_1 = 6.6) and the higher pK_a of the reactive ternary complex (pK_2 = 7.3). The almost identical intrinsic pK_a values for the two mutant enzymes suggest similar solvent accessibility to the Asp27 residue as well as an identical perturbation of its environment in the E·NH·H_2F ternary complex. The apparent pK_a values for k_{cat}/K_M and k_{cat} profiles can be predicted from these intrinsic pK_a values by the relationships from Scheme IV mentioned earlier. The predicted values, 7.5 and 8.7, are in good agreement with the experimentally obtained apparent pK_a values, $pK_a(k_{cat}/K_M)$ = 7.8 and $pK_a(k_{cat})$ = 8.5.

As demonstrated in Figure 4, which shows the pH dependence for the hydride transfer and H_4F dissociation rate constants, the steady-state rate-limiting step changes from H_4F dissociation at low pH to hydride transfer at high pH. The pK_a controlling the overall reaction rate is consequently shifted from pK_a = 7.3 to pK_a = 8.5 (curve 3, Figure 4). The observed steady-state deuterium isotope effects (Table II) are in accord with this change in the rate-limiting step.

Since the crystallographic data (Bolin et al., 1982; Filman et al., 1982) showed that Asp27 is the only ionizing group within the active site of the wild-type *E. coli* DHFR, it follows that this amino acid residue should also be responsible for the pK_a of the E·NH·H_4F ternary complex (pK_3 = 6.6). The importance of Asp27 for substrate protonation has been demonstrated by Howell et al. (1986) by showing that Asn27 or Ser27 mutant DHFR turns over preprotonated substrate but not unprotonated substrate. Although it is debatable how the Asp27 residue assists hydride transfer, it has been proposed that unionized Asp27 delivers a proton to N5 of H_2F through a network of conserved water molecules (Freisheim & Matthews, 1984; Gready, 1985) or acts as a proton relay with the actual proton source being the solvent (Bystroff et al., 1990). An ionized Asp27 residue, on the other hand, may elevate the pK_a value of N5 of enzyme-bound H_2F and act to stabilize the protonated substrate (Gready, 1985; Morrison & Stone, 1988).

Our data (Figure 4) on the pH dependence of H_4F release in the PKRP mutant provides insights regarding the ionization state of Asp27 in catalysis. The observation of differing pK_a values probably associated with differing protein conformations for the substrate ternary complex (E·NH·H_2F; pK_2 = 7.3) and the product ternary complex (E·NH·H_4F; pK_3 = 6.6) suggests that the Asp27 residue is able to ionize during catalysis of hydride transfer. The measurement of two k_{off} values (k_{11} = 20 s^{-1} and k'_{11} = 3.5 s^{-1}; Scheme IV) shows that Asp27 can reprotonate while H_4F is still bound to the active site possibly during the process in which NADPH is exchanged for $NADP^+$. These findings are consistent with the view that this enzyme assists the hydride-transfer step by donating a proton from the carboxyl group of Asp27, which then reequilibrates with solution before the release of H_4F. Since the pK_a of the substrate ternary complex is ca. 0.7 pK_a unit greater than that of the product ternary complex, a higher fraction of Asp27 would be protonated for repetitive turnovers that feature cycling between the two complexes. We cannot unequivocally state that this mutation has not altered the fundamentals of proton transfer, but, insofar as the catalytic properties of PKRP closely resemble those of wild-type DHFR, we view the slight perturbation of pK_a values as providing an opportunity to view the proton-transfer process from Asp27 in the wild-type DHFR.

Another significant advantage associated with the presence of the new hairpin turn is the restoration of the hydride-transfer rate for the PKRP enzyme to levels (k_{hyd} = 530 s^{-1}) comparable to the wild-type values (950 s^{-1} for the *E. coli* enzyme and 450 s^{-1} for the *L. casei* enzyme). This value is observed upon the addition of NADPH to the E·H_2F binary complex. When the reaction is initiated, however, by the addition of H_2F to the E·NADPH binary complex, the hydride-transfer rate is much lower, k_{hyd} = 165 s^{-1}. This is consistent with the conformational hysteresis observed in the steady-state studies that showed the conversion of an NADPH-stabilized enzyme conformer during multiple turnovers to a conformer, or equilibrium state of conformers, with higher activity. The latter state is identical with that stabilized by H_2F, since the reaction rate observed after the new equilibrium has been established is similar to the initial rate observed upon addition of NADPH to the E·H_2F binary complex. The hysteresis seems to reflect a fine tuning of the active-site ensemble of the PKRP enzyme by the binding of H_2F. The absence of such hysteresis in the RYF enzyme suggests that this tuning is associated with the additional mutations made in the loop structure following the αC-helix. The substitution of Gly50 (*E. coli*) with a proline residue and the insertion of a lysine residue at position 52 are intended to introduce a hairpin turn into the enzyme. As mentioned earlier, a cis peptide bond is present between Arg52 and Pro53 of the *L. casei* DHFR but absent in the *E. coli* DHFR sequence. A possible explanation for the hysteresis is that the binding of H_2F to the PKRP enzyme may stabilize a cis peptide bond.

Once in a correct conformation through presence of a hairpin turn the substitute *L. casei* αC-helix can significantly contribute to the orientation of the bound substrate and the cofactor, leading to the restoration of the hydride-transfer rate.

The binding of NADPH to the mutant enzymes exhibits a fast, concentration-dependent phase followed by a much slower, concentration-independent phase. The k_{off} rates are 10–40-fold faster than with the wild-type enzymes. The fast phase consists of two distinguishable, concentration-dependent transients, which can be linearly correlated to NADPH concentration and ascribed to E_1 and E_2 binding (Scheme I). These results are similar to the findings described earlier for MTX binding (Taira & Benkovic, 1988) and NADPH binding (Adams et al., 1989) to the wild-type *E. coli* enzyme. From Scheme I and the data presented in Table IV, it is calculated that, at equilibrium, about 67% of the RYF enzyme is in E_1·NH form, whereas about 82% of the PKRP enzyme is in E_1·NH form. In comparison, about 99% of the wild-type *E. coli* DHFR is in the E_1·NH form at equilibrium (Adams et al., 1989). The binding of H_2F to the PKRP enzyme also follows the same sequence, and about 70% of the enzyme is in E_1·H_2F form. It should be noted that "E_1" represents the conformer that exhibits higher affinity toward the ligands, but E_1·NH and E_1·H_2F may not necessarily designate the same conformer. The implication from the steady-state and pre-steady-state kinetic results is that they possess differing intrinsic reactivities.

Inclusion of the hairpin structure also restores the synergism for H_4F release from the PKRP enzyme. Although the k_{off} values for H_4F from E·H_4F and E·N·H_4F are slightly higher than those for the wild-type *E. coli* DHFR, the dissociation rate constant at pH 6.0 for the release of H_4F from the E·NH·H_4F complex of PKRP returns to a value similar to that for the wild-type enzyme (11 versus 12 s^{-1}). The value of k_{cat} (12 s^{-1}) indicates that E·NH must be the predominant species in the reaction pathway catalyzed by the PKRP enzyme, as is proposed for the *E. coli* as well as the *L. casei* DHFR (Fierke et al., 1987; Andrews et al., 1989).

Our studies on the two mutant DHFRs demonstrate the critical role of the terminal structure of an α-helix. The importance of α-helix terminal boundaries has been discussed in terms of its hydrogen-bonding capacity (Presta & Rose, 1988) and amino acid preference (Richardson & Richardson, 1988). Studies on a single mutation, I50F, in the *E. coli* DHFR conducted in this laboratory (C. R. Wagner and S. J. Benkovic, unpublished data) show a large increase in K_M (H_2F) and a decrease in k_{hyd} to the same extent observed for the RYF enzyme, suggesting that, among the three mutations, the least tolerated change in replacing the αC-helix of the *E. coli* DHFR with that of the *L. casei* DHFR is I50F. The newly incorporated bulky residue may have affected the stability of the C-terminal boundary either by obstructing hydrogen bonding or by dislocation of the α-helix. These unfavorable effects are largely removed by the additional mutations, G51P and an insertion of K52. These two new residues may promote the formation of a cis peptide bond between R53 and P54, which in turn leads to the formation of a hairpin turn. This motif is responsible for placing the αC-helix in an appropriate location and its fine-tuning with regard to substrate binding and product release. Although the αC-helix is an important part of the active site of DHFR, its replacement and further adjustment, as represented by the pentamutant, apparently is not sufficient to shift some of the characteristics of the *E. coli* DHFR, such as the intrinsic pK_a and the off rate for H_4F, toward those of the *L. casei* enzyme. This is in accord with the view that the active-site surface is composed of many amino acid residues that can be interchanged without imposing marked changes in enzymic properties, provided the required secondary structure is achieved.

In conclusion, the replacement of the αC-helix of *E. coli* DHFR with its counterpart of *L. casei* DHFR results in much poorer affinity of the enzyme toward H_2F and a considerable decrease in hydride-transfer rate. The mutation also gives rise to an increase in the k_{off} value for the release of H_4F, which is translated into a parallel increase in the steady-state turnover rate. Moreover, the synergism in the release of H_4F is diminished. In sharp contrast, further incorporation of the hairpin structure attached to the *L. casei* αC-helix into the *E. coli* DHFR results in a mutant enzyme with restored kinetic properties, such as k_{cat}, $K_M(H_2F)$, and k_{hyd}, as well as the synergism in the release of H_4F, to levels similar to those exhibited by the wild-type *E. coli* DHFR. The fortuitous observation of a pH-dependent H_4F release from the PKRP enzyme indicates that the Asp27 residue must undergo ionization during catalysis and can be reprotonated before release of H_4F.

References

Adams, J., Johnson, K., Matthews, R., & Benkovic, S. J. (1989) *Biochemistry 28*, 6611–6618.

Andrews, J., Fierke, C. A., Birdsall, B., Oster, G., Feeney, J., Roberts, G. C. K., & Benkovic, S. J. (1989) *Biochemistry 28*, 5743–5750.

Appleman, J. R., Howell, E. E., Kraut, J., Kuhl, M., & Blakley, R. L. (1988) *J. Biol. Chem. 263*, 9187–9198.

Barshop, B. A., Wrenn, R. F., & Frieden, C. (1983) *Anal. Biochem. 130*, 134–145.

Benkovic, S. J., Fierke, C. A., & Naylor, A. M. (1988) *Science (Washington, D.C.) 239*, 1105–1110.

Birdsall, B., Burgen, A. S. V., & Roberts, G. C. K. (1980) *Biochemistry 19*, 3723–3731.

Blakley, R. L. (1960) *Nature (London) 188*, 231–232.

Bolin, J. T., Filman, D. J., Matthews, D. A., Hamlin, R. C., & Kraut, J. (1982) *J. Biol. Chem. 257*, 13650–13662.

Brown, D. J., & Jacobsen, N. W. (1961) *J. Chem. Soc.* 4413–4420.

Bystroff, C., Oatley, S. J., & Kraut, J. (1990) *Biochemistry 29*, 3263–3277.

Cayley, P. J., Dunn, S. M. J., & King, R. W. (1981) *Biochemistry 20*, 874–879.

Chen, J.-T., Mayer, R. J., Fierke, C. A., & Benkovic, S. J. (1985) *J. Cell Biol. 29*, 73–82.

Chen, J.-T., Taira, K., Tu, C.-P. D., & Benkovic, S. J. (1987) *Biochemistry 26*, 4093–4100.

Cleland, W. W. (1977) *Adv. Enzymol. 45*, 273–387.

Curthoys, H. P., Scott, J. M., & Rabinowitz, J. C. (1972) *J. Biol. Chem. 247*, 1959–1964.

Dunn, S. M. J., & King, R. W. (1980) *Biochemistry 19*, 766–773.

Ellis, K. J., & Morrison, J. F. (1982) *Methods Enzymol. 87*, 405–426.

Fierke, C. A., & Benkovic, S. J. (1989) *Biochemistry 28*, 478–486.

Fierke, C. A., Johnson, K. A., & Benkovic, S. J. (1987) *Biochemistry 26*, 4085–4092.

Filman, D. J., Bolin, J. T., Matthews, D. A., & Kraut, J. (1982) *J. Biol. Chem. 257*, 13663–13672.

Freisheim, J. H., & Matthews, O. A. (1984) in *Folate Antagonists as Therapeutic Agents* (Sirotnak, F. M., Burchall, J. J., Emsiger, W. B., & Montgomery, J. A., Eds.) Vol. 1, pp 69–131, Academic Press, New York.

Gready, J. E. (1985) *Biochemistry 24*, 4761-4766.
Hanahan, D. (1983) *J. Biol. Chem. 166*, 557-580.
Howell, E. E., Villafranca, J. E., Warren, M. S., Oatley, S. J., & Kraut, J. (1986) *Science (Washington, D.C.) 231*, 1123-1128.
Johnson, K. A. (1986) *Methods Enzymol. 134*, 677-705.
Kramer, W., & Fritz, H.-J. (1987) *Methods Enzymol. 154*, 350-367.
Kroeker, W. D., Kowalski, D., & Laskowski, M., Sr. (1976) *Biochemistry 15*, 4463-4467.
Legerski, R. J., & Robberson, D. L. (1985) *J. Mol. Biol. 181*, 297-312.
Mathews, C. K., & Huennekens, F. M. (1960) *J. Biol. Chem. 238*, 3436-3442.
Mayer, R. J., Chen, J.-T., Taira, K., Fierke, C. A., & Benkovic, S. J. (1986) *Proc. Natl. Acad. Sci. U.S.A. 83*, 7718-7720.
Morrison, J. F., & Stone, S. R. (1988) *Biochemistry 27*, 5499-5506.
Murphy, D. J., & Benkovic, S. J. (1989) *Biochemistry 28*, 3025-3031.
Penner, M. H., & Frieden, C. (1985) *J. Biol. Chem. 260*, 5366-5369.
Presta, L. G., & Rose, G. D. (1988) *Science (Washington, D.C.) 240*, 1632-1641.
Richardson, J. S., & Richardson, D. C. (1988) *Science (Washington, D.C.) 240*, 1648-1652.
Sanger, F. (1981) *Science (Washington, D.C.) 214*, 1205-1210.
Seeger, D. R., Cosulich, D. B., Smith, J. M., & Hultquist, M. E. (1949) *J. Am. Chem. Soc. 71*, 1753-1758.
Stone, S. R., & Morrison, J. F. (1982) *Biochemistry 21*, 3757-3765.
Stone, S. R., & Morrison, J. F. (1983) *Biochim. Biophys. Acta 745*, 247-258.
Stone, S. R., & Morrison, J. F. (1984) *Biochemistry 23*, 2753-2758.
Taira, K., & Benkovic, S. J. (1988) *J. Med. Chem. 31*, 129-137.
Taira, K., Fierke, C. A., Chen, J.-T., Johnson, K. A., & Benkovic, S. J. (1987) *Trends Biochem. Sci. (Pers. Ed.) 12*, 275-278.
Villafranca, J. E., Howell, E. E., Voet, D. H., Strobel, M. S., Ogden, R. C., Abelson, J. N., & Kraut, J. (1983) *Science (Washington, D.C.) 222*, 782-788.
Viola, R. E., Cook, P. F., & Cleland, W. W. (1979) *Anal. Biochem. 96*, 334-340.
Volz, K. W., Matthews, D. A., Alden, R. A., Freer, S. T., Corwin, H., Kaufman, B. T., & Kraut, J. (1982) *J. Biol. Chem. 257*, 2528-2536.
Williams, J. W., Morrison, J. F., & Duggleby, R. G. (1979) *Biochemistry 18*, 2567-2573.
Winberg, G., & Hammarskjold, M.-L. (1980) *Nucleic Acids Res. 8*, 253-264.

Designing an Allosterically Locked Phosphofructokinase†

Craig E. Kundrot‡,§ and Philip R. Evans*,‡

Laboratory of Molecular Biology, Medical Research Council, Hills Road, Cambridge CB2 2QH, U.K., and Department of Chemistry and Biochemistry, University of Colorado, Boulder, Colorado 80309-0215

Received July 31, 1990; Revised Manuscript Received October 23, 1990

ABSTRACT: Six site-directed mutants of *Escherichia coli* phosphofructokinase (PFK) were made in an attempt to produce an enzyme "locked" in the inactive or "T"-state. The kinetic properties of the mutants were examined as a function of the substrates fructose 6-phosphate (Fru6P) and ATP, the positive effector GDP, and the negative effector phosphoenolpyruvate (PEP). All mutants exhibited lower activity than wild-type PFK. Three mutants (RS63, LV153, and VT246) had apparent dissociation constants for substrates and effectors similar to those of wild type. One mutant, HN160, had a 10-fold reduced affinity for Fru6P and reduced apparent affinity for the effectors. Two mutants, SN159 and T(GS)156, exhibited hyperbolic kinetics consistent with a "locked" T-state protein. Surprisingly, T(GS)156 showed hyperbolic activation in response to the physiological inhibitor PEP. The mutant PFK properties are discussed in terms of the PFK structure. These results suggest that the kinetic properties of PFK are sensitive to interactions in the homotropic interface; residues 156-160 in particular are critical in mediating the interactions between effector and active sites and in the T to R quaternary transition.

Phosphofructokinase (PFK) catalyzes the formation of fructose 1,6-bisphosphate and ADP from fructose 6-phosphate (Fru6P) and ATP and is the main regulatory enzyme in glycolysis. The enzyme from *Escherichia coli* exhibits Michaelis-Menten kinetics with respect to ATP but cooperative kinetics with respect to Fru6P, the allosteric activator ADP, and the allosteric inhibitor phosphoenolpyruvate (PEP). The kinetics of *E. coli* PFK were thoroughly studied by Blangy et al. (1968) and were the first enzyme kinetics shown to fit to the Monod-Wyman-Changeaux (Monod et al., 1965) model of cooperativity (MWC). Blangy et al. showed that the kinetics fit well to a two-state "K-system" model, in which PFK exists in states with high (R) and low (T) affinity for Fru6P. This model contrasts with a "V-system" model in which the different forms of the enzyme have different k_{cat} values rather than different binding constants. The MWC model is used in this paper as the conceptual framework for understanding wild-type and mutant PFKs, although the truth is undoubtedly

† C.E.K. is a Fellow of the Jane Coffin Childs Memorial Fund for Medical Research, and this work was supported in part by the Jane Coffin Childs Memorial Fund for Medical Research.
‡ Medical Research Council.
§ University of Colorado.

0006-2960/91/0430-1478$02.50/0 © 1991 American Chemical Society